Tropical Journal of Pharmaceutical Research June 2018; 17 (6): 1095-1110
ISSN: 1596-5996 (print); 1596-9827 (electronic)

Available online at http://www.tjpr.org
http://dx.doi.org/10.4314/tjpr.v17i6.17

Original Research Article

Network pharmacology and UPLC-Q-TOF/MS studies on the anti-arthritic mechanism of *Pterocephalus hookeri*

Ce Tang[1], Hai-Jiao Li[1], Gang Fan[1], Ting-Ting Kuang[1], Xian-Li Meng[1], Zhong-Mei Zou[2], Yi Zhang[1]*

[1]College of Ethnic Medicine, Chengdu University of Traditional Chinese Medicine, Chengdu 611137, [2]Institute of Medicinal Plant Development, Chinese Academy of Medical Sciences and Peking Union Medical College, Beijing 100193, China

For correspondence: **Email: 1175332408@qq.com; **Tel:** +86 28 61800074*

Sent for review: 17 February 2018 *Revised accepted: 26 May 2018*

Abstract

***Purpose:** To investigate the mechanism underlying the anti-arthritic properties of Pterocephalus hookeri used for treatment of rheumatoid arthritis (RA).*
***Methods:** Aqueous methanol extract of P. hookeri was analyzed using UPLC-Q-TOF/MS, a Waters Acquity UPLCR BEH C18 column (2.1 × 100 mm, 1.7 μm) and gradient elution with acetonitrile-formic acid-water. Targets and related pathways were predicted by PharmMapper database and Molecule Annotation System, respectively. The network was built with Cytoscape software.*
***Results:** Forty compounds were identified, comprising 17 iridoid glycosides, 7 phenolic acids, 13 triterpenes, and 3 other compounds. A total of 38 targets and 44 pathways associated with RA were obtained. These involved mainly MAPK signaling pathway, adherens junction, and colorectal cancer.*
***Conclusion:** These results from network pharmacology suggest that P. hookeri exerts therapeutic effect on RA via multiple components, multiple targets and multiple pathways.*

***Keywords:** Pterocephalus hookeri, Rheumatoid arthritis, UPLC-Q-TOF/MS, Chemical composition, Network pharmacology*

INTRODUCTION

Rheumatoid arthritis (RA) is a systemic autoimmune disease which occurs in three stages: chronic, progressive, and aggressive arthritis, eventually leading to joint deformity and loss of function. Thus, RA has a high frequency of disability [1]. In Tibetan medicine, RA is called “zhen bu” disease [2], and available data show that the treatment efficacy of Tibetan medicine for RA is up to 94.6 % [3,4].

Previous studies have confirmed that the major chemical components of *P. hookeri* include iridoid glycosides, triterpenoid saponins, and phenolic acids [5,6]. A survey of ancient literature revealed that *P. hookeri* was frequently used in the treatment of RA [7]. Some recent studies have shown that aqueous and ethanolic extracts of *P. hookeri* have anti-inflammatory, anti-RA, and analgesic effects [8,9]. Although there are several studies on *P. hookeri*, its mechanism of action on RA has not received much attention.

Recently, network-based analyses have emerged as powerful tools for elucidating the multiple and active components of extracts, as well as their mechanisms of action [10]. A new approach is provided by network pharmacology for the study of activities of multiple components and pharmacological mechanisms in traditional medicine.

The purpose of the research was to use network pharmacology and UPLC-Q-TOF/MS to unravel the active ingredients of *P. hookeri*, their targets, and the mechanism involved in the anti-RA effect of the plant.

EXPERIMENTAL

Materials and reagents

Acetonitrile and formic acid (HPLC grade) were supplied by Merck (Darmstadt, Germany) and Fluka (Buchs, Steinheim, Germany), respectively. Distilled water used for UPLC-Q-TOF/MS was acquired using the Milli-Q system (Millipore, France), while *P. hookeri* was purchased from Ganzi Tibetan Hospital in Sichuan, China. The standards (~98 % purity) of loganic acid (3), chlorogenic acid (4), sweroside (9), loganin (10), 6-apiofuranosylsweroside (12), 3,4-dicaffeoylquinic acid (15), 3,5-dicaffeoylquinic acid (16), 4,5-dicaffeoylquinic acid (18), ursolic acid (39), and oleanolic acid (40) were supplied by the National Institute for Food and Drug Control (Beijing, China) or Chengdu Must Bio-Technology Co., Ltd. (Chengdu, Ching). Sylvestroside I (17), cantleyoside (19), triplostoside A (25), dipsanosides B (26), and dipsanosides A (27) were acquired from *P. hookeri* by in previous studies [11,12].

Sample preparation

Powered *P. hookeri* (2.0 g) was accurately weighed and added to 50 mL of 70 % aqueous methanol. The mixture was subjected to ultrasonic extraction for 30 min, and filtered. The residue was washed with a small amount of 70 % aqueous methanol, and the combined filtrate was concentrated and dissolved in the same solvent. The concentrated solution was transferred to a 10 mL bottle, and 70 % methanol was added to the mark. The supernatant was centrifuged at 14000 rpm for 15 min and filtered through a 0.22 μm microporous membrane.

UPLC chromatography

UPLC was performed in a 100 mm × 2.1 mm, 1.7 μm Waters Acquity UPLC^{R} BEH C18 column (Waters Corp., Milford, USA). The mobile phase was composed of acetonitrile (A), and water (B) each containing 0.1 % formic acid. The linear gradient program was performed as follows: 5 - 12 % B for 0 - 7 min; 12 - 17 % B for 7 - 8 min; 17 % B for 8 - 13 min; 17 - 25 % B for 13 - 20 min; 25 - 46 % B for 20 - 23 min; 46 % B for 23 - 26 min; 46 - 60 % B for 23 - 32 min; 60 - 95 % B for 32 - 35 min, and 95 % B for 35 - 36 min. Flow rate, 0.4 mL/min; injection volume, 2 μL; column temperature, 40 ^{o}C.

Mass spectrometry

Waters SYNAPT G2HDMS system of ion source was used for electrospray ionization (ESI). Scanning was done at positive (ESI+) and negative (ESI-) ion modes, with nitrogen as atomization and conical gas. The source temperature and cone gas flow rate were 100 °C and 40 L/h, respectively. Desolvation temperature and gas flow rate were 350 °C and 800 L/h, respectively. Other MS conditions used were sampling cone voltage of 40V, extraction cone voltage of 4V, capillary voltages of 3.0 kV (ESI+) and 2.5 kV (ESI-), scan time and inter scan time (0.3 s and 0.02 s, respectively), and mass-to-charge ratio, *m*/*z* of 50 - 1700. Leucine-enkephalin (0.5 μg/mL) at a flow velocity of 5 μL/min, was used for calibration of mass number (*m*/*z* 556.2771 for ESI+, and *m*/*z* 554.2615 for ESI-).

Prediction and screening of targets

ChemBio Office 2014 software was used to draw the structures of the compounds. These were converted to 3D forms with ChemBio3D ultra software, and stored in mol2 format. Then, in order to predict the potential target, chemical components were imported into the PharmMapper website (http://lilab.ecust.edu.cn/pharmmapper/) for potential target prediction analysis. The first 10 targets of each compound were selected for follow-up study.

Prediction and screening of pathways

The targets obtained were introduced into the Bio database (http://bioinfo.capitalbio. com/mas3/) and then screened for pathways that met the criterion of $p < 0.01$.

Construction of network

Cytoscape software was used to construct compound-target-pathway networks with chemical constituents, predicted targets and pathways.

RESULTS

Compositions of *P. hookeri*

Data on the ESI+ and ESI- modes are shown in Figure 1. It was found that ESI- mode provided a neater MS fragmentation and sharper peak shapes than ESI+. However, it was easier to find the quasi-molecular ion peaks of compounds with combination of positive and negative ions. Using relative retention times, exact masses, MS fragments, standards, and references, 40 compounds were identified or elucidated with the information shown in Figure 1, Figure 2, Table 1.

Compounds of iridoid glycosides have variety of activities, such as anti-inflammatory [8], anti-RA [2], and the anti-tumor [24] activities. A total of 17 (**1, 3, 7-12, 17, 19-21, 23-27**) compounds were identified at the same time in ESI+ and ESI- modes. A glucose unit (Glc, 162 Da) was a representative fragment during a neutral loss scan of all iridoid glycosides. Taking peak **3** as an example, the quasi-molecular ions $[2M+Na-2H]^-$ at *m/z* 773.2469, $[2M-H]^-$ at *m/z* 751.2656, and $[M-H]^-$ at *m/z* 375.1281, indicated that the formula of the compound was $C_{16}H_{24}O_{10}$. Figure 3A indicates that $[M-H]^-$ of peak 3 got the ions at *m/z* 213.0759 and 169.0859 by losing 162 Da (Glc) and 44 Da (CO_2). Besides, the ions at *m/z* 113.0239 and 151.0752 were generated by the characteristic retro-Diels-Alder (RDA) cleavage loss of C_3H_4O (56 Da) and H_2O (18 Da), respectively from the fragment ion at *m/z* 169.0859 [15]. As a consequence, by comparison with standard, peak **3** was confirmed as loganic acid. The proposed fragmentation pathway of loganic acid (peak **3**) is displayed in Figure 3B.

Seven (**2, 4-6, 15, 16, 18**) compounds were identified as phenolic acids from *P. hookeri* in the ESI+ and ESI- modes. Peak **4** generated a $[2M-H]^-$ ion at *m/z* 707.1810, $[M+Na-2H]^-$ ion at *m/z* 375.0866, and $[M-H]^-$ ion at *m/z* 353.0866, indicated that the formula of the compound was $C_{16}H_{18}O_9$. The $[M-H-C_9H_6O_3]^-$ ion at *m/z* 191.0560, and [caffeic acid-H]$^-$ ion at *m/z* 179.0350 showed that the compound structure contained a quinic acid and caffeic acid. Comparing with standard, peak **4** was unambiguously confirmed as chlorogenic acid. Peaks **2** and **6** had uniform quasi-molecular ion at *m/z* 353, which indicates that these two compounds were isomeric with **4**. It was easy to distinguish peaks **2** and **6** using literature reports and their relative retention times [14]. Peaks **15**, **16**, and **18** were had the same quasi-molecular and fragment ions, indicating that these three compounds were isomeric. On the basis of comparisons with standards, and literature reports, the three peaks were confirmed as 3,4-dicaffeoylquinic acid, 3,5-dicaffeoylquinic acid, and 4,5-dicaffeoylquinic acid. The derivation of the fragmentation pathway of 3,5-dicaffeoylquinic acid is shown in Figure 4B.

The other major chemical constituents of *P. hookeri* were triterpenes. A triterpene molecule is an aglycone formed after the removal the removal of one or more sugar moieties from a triterpene glycoside. The most common sugar moieties in triterpenes are glucose (Glc), rhamnose (Rha), and xylose (Xyl), and they are linked to the aglycone through O-glycosidic linkages in positions 3 and 28. Therefore, the loss of 162 Da (Glc), 132 Da (Rha), and 146 Da (Xyl) in MS data are characteristic for triterpenes. The triterpenes differ in type and amount of sugar present. Thirteen triterpenes (**28-40**) were identified. For example, peak **35** exhibited ions at *m/z* 1033.5337 ($[M+Na-2H]^-$) and 1011.5532 ($[M-H]^-$), corresponding to the molecular formula $C_{52}H_{84}O_{19}$. The MS spectrum of peak **35** gave four major fragment ions at *m/z* 865.4962 ($[M-H-Rha]^-$), 733.4523 ($[M-H-Rha-Xyl]^-$), 587.3956 ($[M-H-2Rha-Xyl]^-$), and 455.3532 ($[M-H-2Rha-2Xyl]^-$), demonstrating the presence of two rhamnose and xylose residues. From references, peak **35** was confirmed as triploside G. The proposed fragmentation pathway of triploside G (peak **35**) is shown in Figure 5B.

Apart from iridoid glycosides, triterpenes, and phenolic acids, three other compounds (**13, 14, 22**) were identified from *P. hookeri*. Additional information about these compounds and their chemical constitutions are shown in Table 1 and Figure 2, respectively.

Network pharmacology

A total of 38 targets were obtained by importing 40 chemical compositions predicted to be absorbable into the PharmMapper database for directional docking (Table 2).These targets were then imported into the Molecule Annotation System, which resulted 57 pathways regulated by *P. hookeri* with significant differences ($p < 0.05$). Forty-four of these pathways that met the criterion of $P < 0.01$ (Table 3).

Cytoscape software was used to construct a pharmacology network of *P. hookeri* to generate the correlations of chemical components, targets,

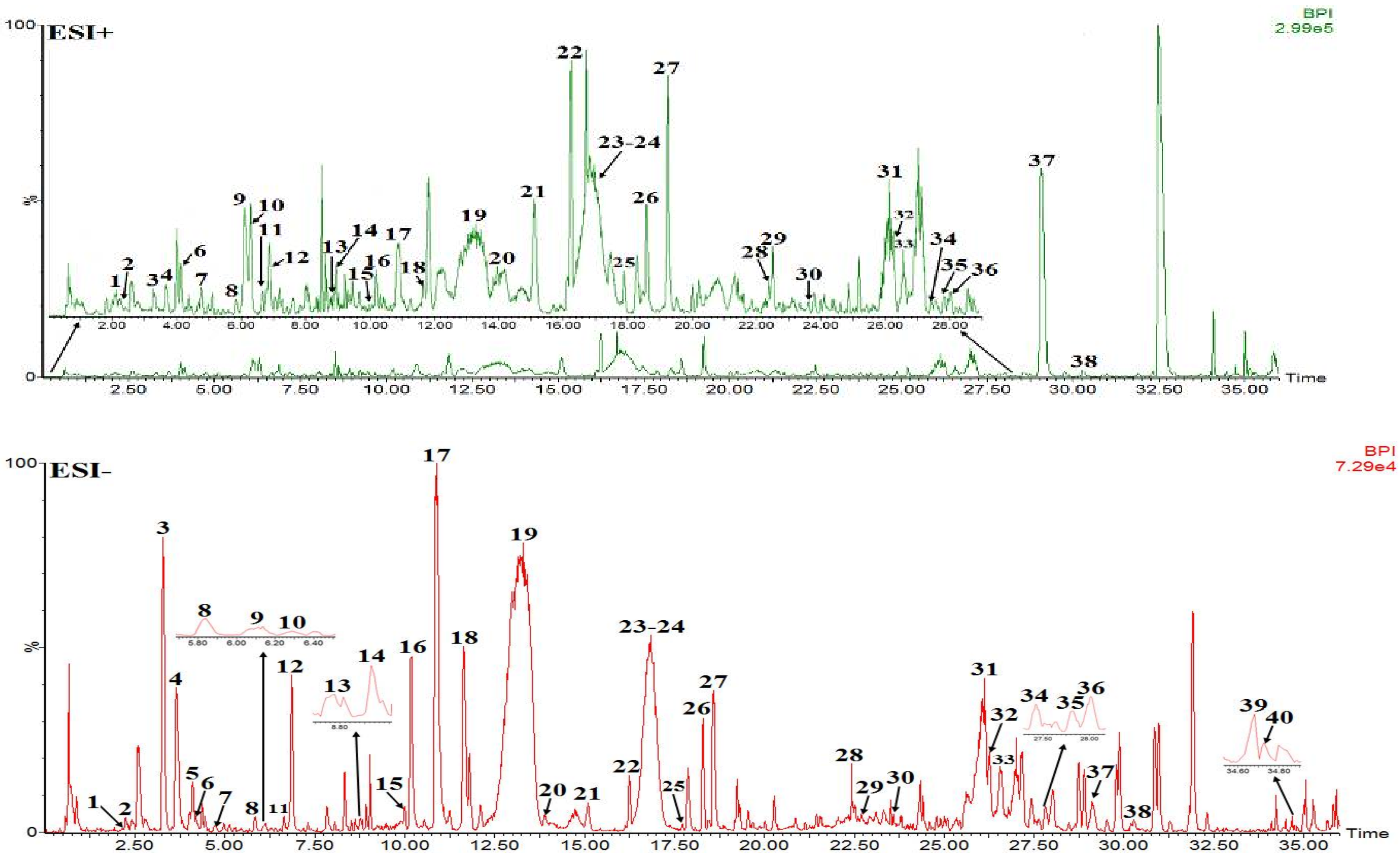

Figure 1: The base peak ion current chromatogram of *P. hookeri* in ESI+ and ESI- modes

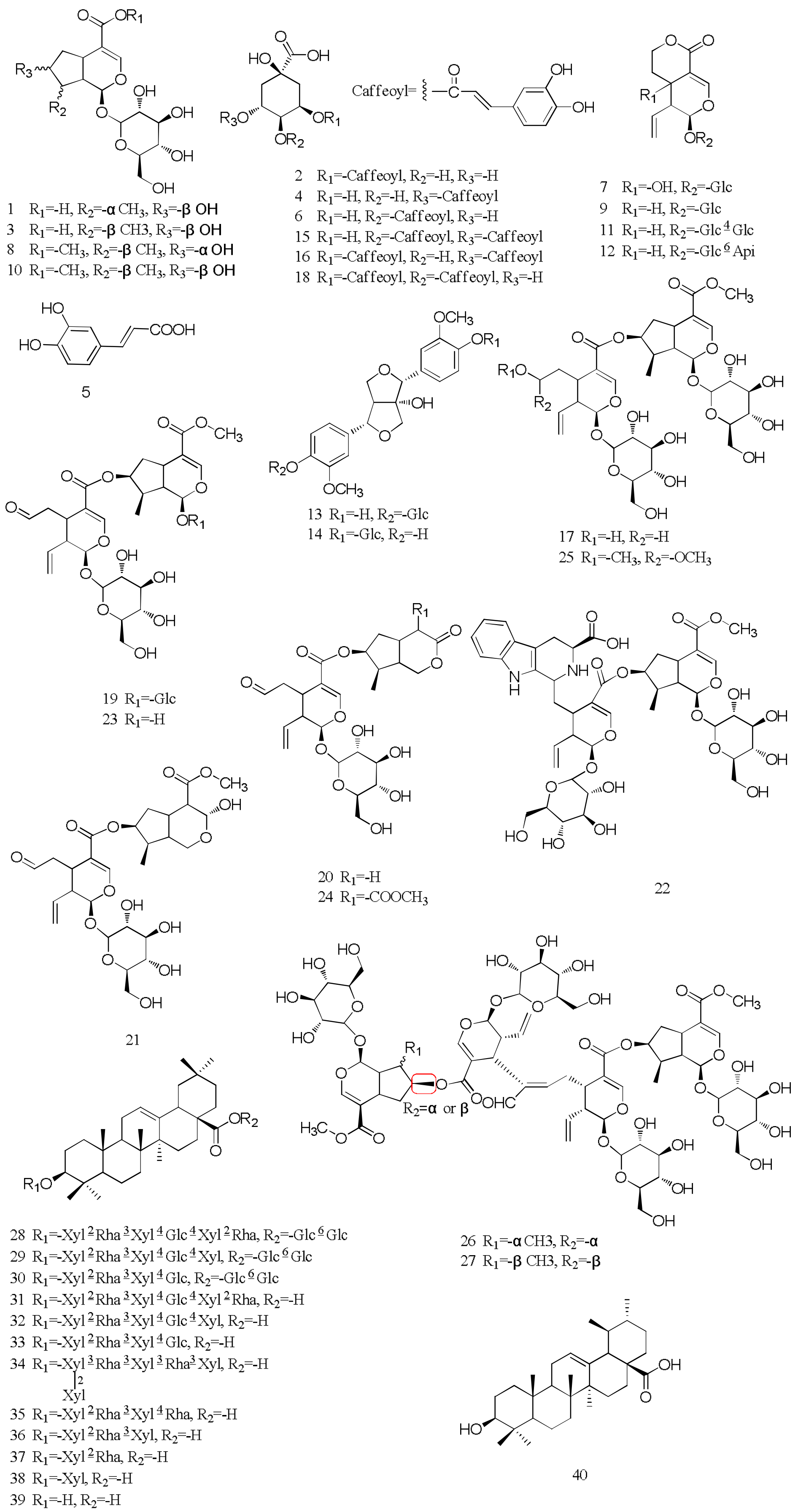

Figure 2: Chemical structures of compounds identified

Table 1: ESI-TOF/MS data for compounds identified from *P. hookeri*

No.	T_R (min)	Formula	MS (error in ppm)	Fragment ions	Identification	Ref.
1b	2.17	$C_{16}H_{24}O_{10}$	375.1294 [M-H]$^-$ (0.8)	397.1082 [M+Na-2H]$^-$, 213.0768 [M-H-Glc]$^-$, 169.0846 [M-H-Glc-CO_2]$^-$	8-*epi*-loganin acid	[13]
2b	2.25	$C_{16}H_{18}O_9$	353.0870 [M-H]$^-$ (-0.8)	173.0441 [M-H-$C_9H_6O_3$-H_2O]$^-$, 161.0235 [$C_9H_8O_4$-H-H_2O]$^-$, 135.0445 [$C_9H_8O_4$-H-CO_2]$^-$	Neochlorogenic acid	[14]
3a	3.29	$C_{16}H_{24}O_{10}$	375.1298 [M-H]$^-$ (-2.7)	773.2469 [2M+Na-2H]$^-$, 751.2656 [2M-H]$^-$, 213.0759 [M-H-Glc]$^-$, 169.0859 [M-H-Glc-CO_2]$^-$, 151.0752 [M-H-Glc-CO_2-H_2O]$^-$, 113.0239 [M-H-Glc-CO_2-C_3H_4O]$^-$	Loganic acid	[13]
4a	3.64	$C_{16}H_{18}O_9$	353.0866 [M-H]$^-$ (-2.0)	729.1613 [2M+Na-2H]$^-$, 707.1810 [2M-H]$^-$, 375.0866 [M+Na-2H]$^-$, 191.0560 [M-H-$C_9H_6O_3$]$^-$, 179.0350 [$C_9H_8O_4$-H]$^-$	Chlorogenic acid	[14]
5b	4.10	$C_9H_8O_4$	179.0351 [M-H]$^-$ (3.9)	201.0152 [M+Na-2H]$^-$, 135.0452 [M-H-CO_2]$^-$	Caffeic acid	[13]
6b	4.14	$C_{16}H_{18}O_9$	353.0866 [M-H]$^-$ (-2.0)	375.0877 [M+Na-2H]$^-$, 191.0556 [M-H-$C_9H_6O_3$]$^-$, 179.0345 [$C_9H_8O_4$-H]$^-$, 173.0452 [M-H-$C_9H_6O_3$-H_2O]$^-$	Cryptochlorogenic acid	[14]
7b	4.74	$C_{16}H_{22}O_{10}$	373.1124 [M-H]$^-$ (-2.9)	769.2156 [2M+Na-2H]$^-$, 747.2343 [2M-H]$^-$, 211.0236 [M-H-Glc]$^-$, 167.0701 [M-H-Glc-CO_2]$^-$	Swertimarin	[13]
8b	5.84	$C_{17}H_{26}O_{10}$	389.1462 [M-H]$^-$ (3.6)	227.0904 [M-H-Glc]$^-$	7-*epi*-loganin	[13]
9a	6.10	$C_{16}H_{22}O_9$	357.1201 [M-H]$^-$ (4.2)	715.2451 [2M-H]$^-$, 403.1239 [M-H+HCOOH]$^-$, 297.1115 [M-H-$C_2H_4O_2$]$^-$, 195.0660 [M-H-Glc]$^-$, 125.0242 [M-H-Glc-C_4H_6O]$^-$	Sweroside	[15]
10a	6.29	$C_{17}H_{26}O_{10}$	779.2971 [2M-H]$^-$ (-0.4)	801.1882 [2M+Na-2H]$^-$, 435.1503 [M-H+HCOOH]$^-$, 227.0926 [M-H-Glc]$^-$, 209.0838 [M+H-Glc-H_2O]$^-$,	Loganin	[13]
11b	6.65	$C_{22}H_{32}O_{14}$	519.1710 [M-H]$^-$ (-0.8)	1039.3473 [2M-H]$^-$, 357.1199 [M-H-Glc]$^-$, 195.0662 [M-H-Glc-Glc]$^-$	Dipsanosides H	[16]
12ab	6.85	$C_{21}H_{30}O_{13}$	489.1609 [M-H]$^-$ (0.2)	979.3309 [2M-H]$^-$, 535.1652 [M-H+HCOOH]$^-$, 357.1214 [M-H-Api]$^-$, 339.0517 [M-H-Api-H_2O]$^-$, 195.0657 [M-H-Api-Glc]$^-$, 149.0452 [M-H-Api-Glc-H_2O-CO]$^-$, 125.0238 [M-H-Api-Glc-C_4H_6O]$^-$	6'-apiofuranosylsweroside	[16]
13	8.80	$C_{26}H_{32}O_{12}$	535.1815 [M-H]$^-$ (-0.2)	557.1970 [M+Na-2H]$^-$, 373.1283 [M-H-Glc]$^-$	8-hydroxylpinoresionl-4'-glucoside	[10]
14	8.94	$C_{26}H_{32}O_{12}$	535.1865 [M-H]$^-$ (5.0)	557.2025 [M+Na-2H]$^-$, 373.1291 [M-H-Glc]$^-$	8'-hydroxylpinoresionl-4-glucoside	[10]
15ab	10.01	$C_{25}H_{24}O_{12}$	515.1208 [M-H]$^-$ (3.5)	1053.2207 [2M+Na-2H]$^-$, 537.1027 [M+Na-2H]$^-$, 353.0879 [M-H- $C_9H_6O_3$]$^-$, 191.0549 [M-H-2$C_9H_6O_3$]$^-$	3,4-dicaffeoylquinic acid	[14]
16ab	10.19	$C_{25}H_{24}O_{12}$	515.1183 [M-H]$^-$ (-1.4)	1031.2461 [2M-H]$^-$, 353.0869 [M-H- $C_9H_6O_3$]$^-$, 191.0557 [M-H-2 $C_9H_6O_3$]$^-$	3,5-dicaffeoylquinic acid	[14]
17a	10.89	$C_{33}H_{48}O_{19}$	747.2701 [M-H]$^-$ (-1.5)	1495.5585 [2M-H]$^-$, 585.2175 [M-H-Glc]$^-$, 423.1235 [[M-H-Glc-Glc]$^-$	Sylvestroside I	[10]
18ab	11.70	$C_{25}H_{24}O_{12}$	515.1197 [M-H]$^-$ (1.4)	1053.2296 [2M+Na-2H]$^-$, 1031.2493 [2M-H]$^-$, 537.1018 [M+Na-2H]$^-$, 353.0872 [M-H-$C_9H_6O_3$]$^-$, 191.0549 [M-H-2$C_9H_6O_3$]$^-$	4,5-dicaffeoylquinic acid	[14]

Table 1: ESI-TOF/MS data for compounds identified from *P. hookeri* (*contd*)

No.	T_R (min)	Formula	MS (error in ppm)	Fragment ions	Identification	Ref.
19a	13.34	$C_{33}H_{46}O_{19}$	745.2576 $[M-H]^-$ (2.8)	1491.5344 $[2M-H]^-$, 583.2040 $[M-H-Glc]^-$, 421.1163 $[M-H-Glc-Glc]^-$	Cantleyoside	[11]
20	13.90	$C_{25}H_{34}O_{12}$	525.1973 $[M-H]^-$ (0.2)	1051.4105 $[2M-H]^-$, 571.2026 $[M-H+HCOOH]^-$, 363.1512 $[M-H-Glc]^-$	Laciniatoside II	[17]
21	15.10	$C_{27}H_{38}O_{14}$	585.2172 $[M-H]^-$ (-1.9)	631.2221 $[M-H+HCOOH]^-$, 423.1652 $[M-H-Glc]^-$	Laciniatoside I	[17]
22b	16.24	$C_{44}H_{56}N_2O_{20}$	933.3507 $[M+H]^+$ (0.2)	771.2957 $[M+H-Glc]^+$, 609.2066 $[M+H-Glc-Glc]^+$	Pterocephaline	[18]
23	16.71	$C_{27}H_{36}O_{14}$	583.2030 $[M-H]^-$ (0.5)	1189.3997 $[2M+Na-2H]^-$, 421.1485 $[M-H-Glc]^-$	Sylvestroside III	[17]
24	16.84	$C_{27}H_{36}O_{14}$	583.2030 $[M-H]^-$ (0.5)	1189.3986 $[2M+Na-2H]^-$, 421.1462 $[M-H-Glc]^-$	Sylvestroside VI	[17]
25a	17.72	$C_{35}H_{52}O_{20}$	791.2967 $[M-H]^-$ (-0.9)	629.2448 $[M-H-Glc]^-$	Triplostoside A	[14]
26a	18.28	$C_{66}H_{90}O_{37}$	1473.5153 $[M-H]^-$ (4.8)	1311.4646 $[M-H-Glc]^-$, 1131.3984 $[M-H-2Glc-H_2O]^-$, 969.2977 $[M-H-3Glc-H_2O]^-$, 825.2862 $[M-H-4Glc]^-$	Dipsanosides B	[14]
27a	18.58	$C_{66}H_{90}O_{37}$	1473.5129 $[M-H]^-$ (3.1)	1311.4545 $[M-H-Glc]^-$, 1149.3488 $[M-H-2Glc]^-$, 969.2973 $[M-H-3Glc -H_2O]^-$, 807.2715 $[M-H-4Glc-H_2O]^-$	Dipsanosides A	[14]
28	22.44	$C_{75}H_{122}O_{38}$	1629.7534 $[M-H]^-$ (-0.1)	1305.6500 $[M-H-2Glc]^-$, 1159.6040 $[M-H-2Glc-Rha]^-$, 1027.5486 $[M-H-2Glc-Rha-Xyl]^-$, 865.4760 $[M-H-3Glc-Rha-Xyl]^-$, 733.4683 $[M-H-3Glc-Rha-2Xyl]^-$, 587.3968 $[M-H-3Glc-2Rha-2Xyl]^-$, 455.3522 $[M-H-3Glc-2Rha-3Xyl]^-$	Hookerosides C	[19]
29	22.50	$C_{69}H_{112}O_{34}$	1483.7013 $[M-H]^-$ (3.8)	1159.5927 $[M-H-2Glc]^-$, 1027.5481 $[M-H-2Glc -Xyl]^-$, 865.4907 $[M-H-3Glc-Xyl]^-$, 733.4633 $[M-H-3Glc-2Xyl]^-$, 587.3981 $[M-H-3Glc-Rha-2Xyl]^-$, 455.3550 $[M-H-3Glc-Rha-3Xyl]^-$	Hookerosides B	[19]
30	23.60	$C_{64}H_{104}O_{30}$	1351.6509 $[M-H]^-$ (-1.8)	1027.5470 $[M-H-2Glc]^-$, 865.4976 $[M-H-3Glc]^-$, 733.4747 $[M-H-3Glc-Xyl]^-$, 587.3919 $[M-H-3Glc-Xyl-Rha]^-$, 455.3521 $[M-H-3Glc-2Xyl-Rha]^-$	Hookerosides A	[19]
31	26.07	$C_{63}H_{102}O_{28}$	1305.6544 $[M-H]^-$ (5.0)	1327.6381 $[M+Na-2H]^-$, 1159.5917 $[M-H-Rha]^-$, 1027.5478 $[M-H-Rha-Xyl]^-$, 865.4871 $[M-H-Rha-Xyl-Glc]^-$, 733.4586 $[M-H-Rha-2Xyl-Glc]^-$, 587.3935 $[M-H-2Rha-2Xyl-Glc]^-$, 455.3524 $[M-H-2Rha-3Xyl-Glc]^-$	Hookerosides D	[19]
32	26.25	$C_{57}H_{92}O_{24}$	1159.5923 $[M-H]^-$ (2.0)	1181.5713 $[M+Na-2H]^-$, 1027.5490 $[M-H-Xyl]^-$, 865.4960 $[M-H-Xyl-Glc]^-$, 733.4566 $[M-H-2Xyl-Glc]^-$, 587.4064 $[M-H-Rha-2Xyl-Glc]^-$, 455.3505 $[M-H-Rha-3Xyl-Glc]^-$	Oleanolic acid 3-Xyl (1→4)-Glc(1→4)-Xyl(1→3)-Rha(1→2)-Xyl	[19]
33	26.55	$C_{52}H_{84}O_{20}$	1027.5485 $[M-H]^-$ (0.7)	1049.5216 $[M+Na-2H]^-$, 865.4986 $[M-H-Glc]^-$, 733.4459 $[M-H-Glc-Xyl]^-$, 587.3894 $[M-H-Glc-Xyl-Rha]^-$, 455.3520 $[M-H-Glc-2Xyl-Rha]^-$	Oleanolic acid 3-Glc (1→4)-Xyl(1→3)-Rha(1→2)-Xyl	[19]
34	27.43	C62H100O27	1275.6399 [M-H]- (2.0)	1297.6207 [M+Na-2H]-, 1143.5941 [M-H-Xyl]-, 997.5147 [M-H-Xyl-Rha]-, 865.5060 [M-H-2Xyl-Rha]-, 719.4508 [M-H-2Xyl-2Rha]-, 587.3959 [M-H-3Xyl-2Rha]-, 455.3520 [M-H-4Xyl-2Rha]-	Rivularicin	[20]
35b	27.82	C52H84O19	1011.5532 [M-H]- (0.3)	1033.5337 [M+Na-2H]-, 865.4962 [M-H-Rha]-, 733.4523 [M-H-Rha-Xyl]-, 587.3956 [M-H-2Rha-Xyl]-, 455.3532 [M-H-2Rha-2Xyl]-	Triploside G	[21]

Table 1: ESI-TOF/MS data for compounds identified from *P. hookeri* (*contd*)

No.	T_R (min)	Formla	MS (error in ppm)	Fragment ions	Identification	Ref.
36	28.00	$C_{46}H_{74}O_{15}$	865.4957 $[M\text{-}H]^-$ (0.9)	887.4765 $[M+Na\text{-}2H]^-$, 733.4520 $[M\text{-}H\text{-}Xyl]^-$, 587.3954 $[M\text{-}H\text{-}Rha\text{-}Xyl]^-$, 455.3538 $[M\text{-}H\text{-}Rha\text{-}2Xyl]^-$	Oleanolic acid 3-Xyl(1→3)- Rha(1→2)-Xyl	[19]
37	29.15	$C_{41}H_{66}O_{11}$	733.4531 $[M\text{-}H]^-$ (0.5)	587.3969 $[M\text{-}H\text{-}Rha]^-$, 455.3524 $[M\text{-}H\text{-}Rha\text{-}Xyl]^-$	giganteaside D	[19]
38	30.33	$C_{35}H_{56}O_7$	587.3927 $[M\text{-}H]^-$ (-3.6)	455.3567 $[M\text{-}H\text{-}Xyl]^-$	songoroside A	[19]
39a	34.68	$C_{30}H_{48}O_3$	455.3539 $[M\text{-}H]^-$ (3.1)		Oleanolic acid	[22]
40a	34.73	$C_{30}H_{48}O_3$	455.3510 $[M\text{-}H]^-$ (-3.3)		Ursolic acid	[22]

a, Identified with standards; b, The first discovery of the compound from *P. hookeri*

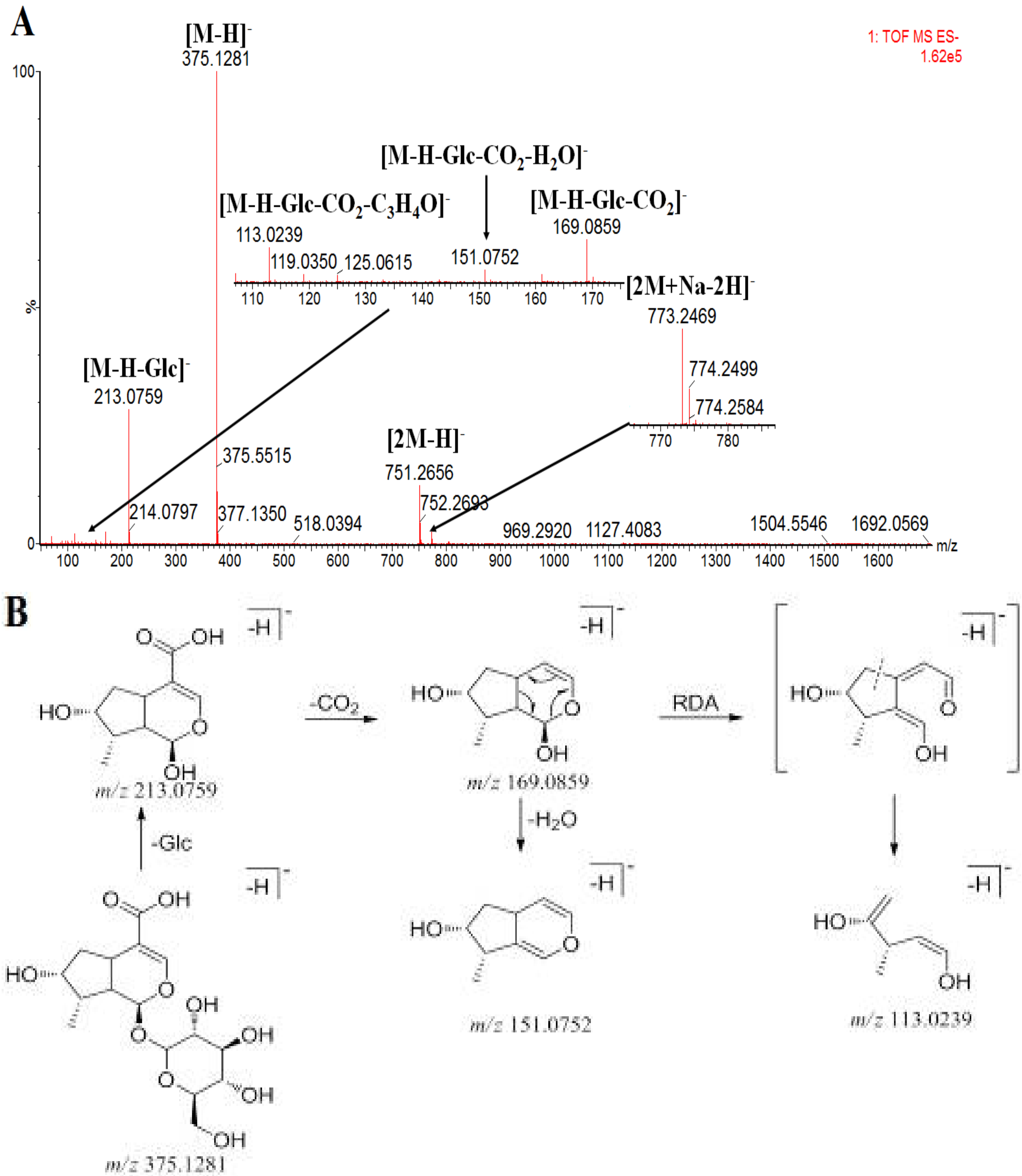

Figure 3: MS diagram (ESI-) and ions fragmentation pathways of loganic acid (3)

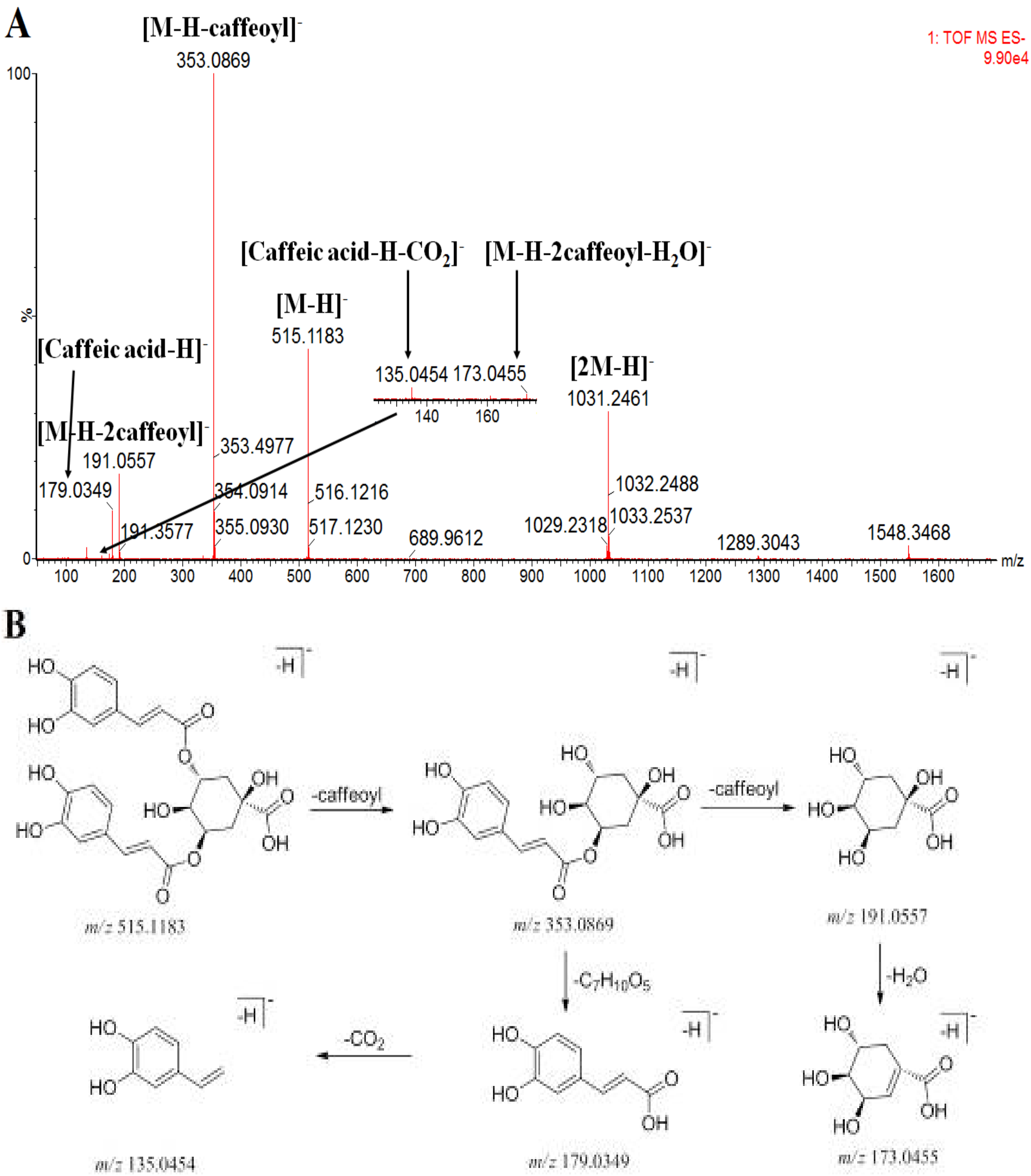

Figure 4: MS diagram (ESI-) and ions fragmentation pathways of 3,5-dicaffeoylquinic acid (16)

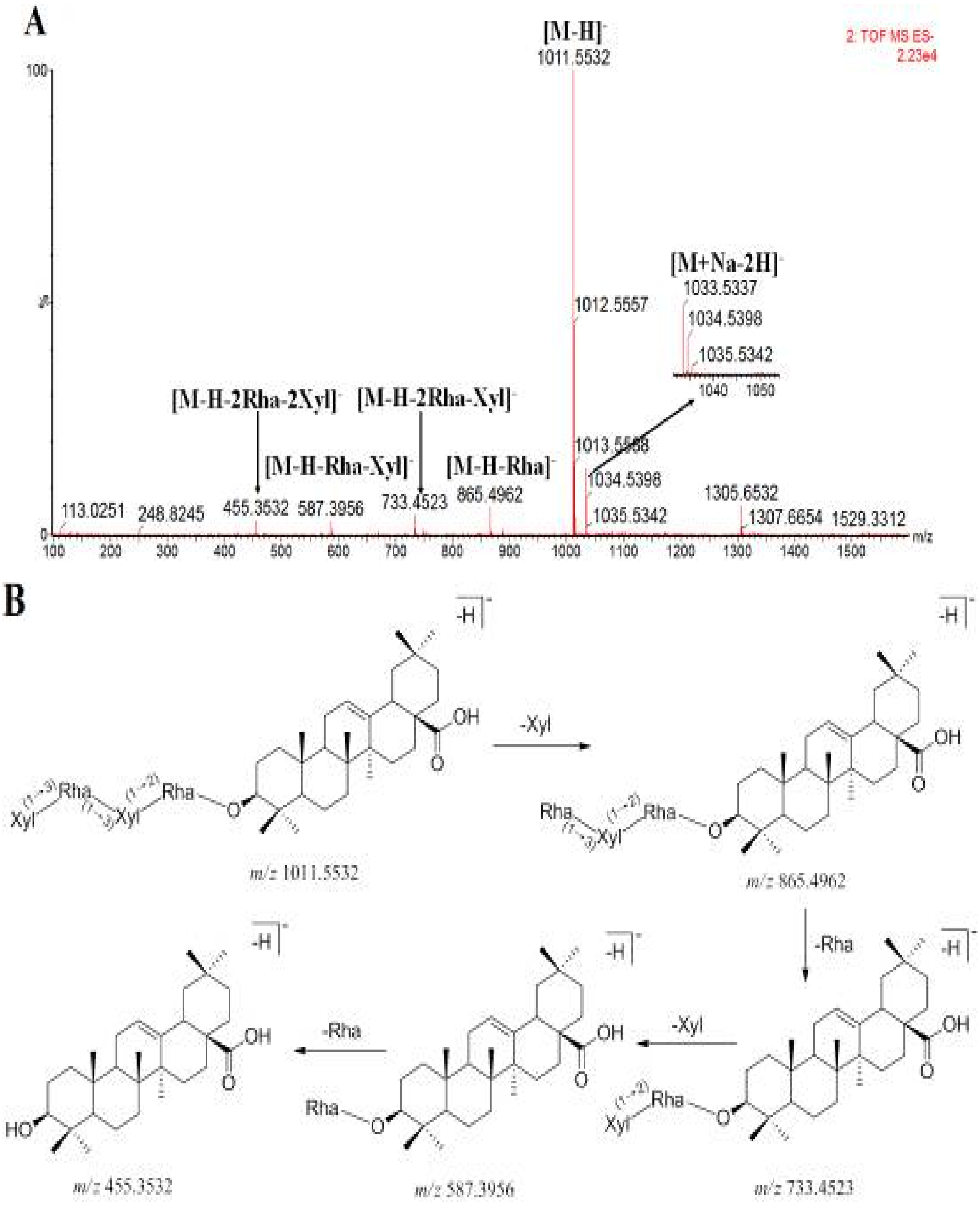

Figure 5: MS diagram (ESI-) and ions fragmentation pathways of triploside G (35)

Table 2: Information on potential targets from compounds of *P. hookeri*

No.	Gene	Protein	Compound
1	CA2	Carbonic anhydrase 2	3, 4, 5, 6, 8, 9, 10, 11, 12, 14, 15, 17, 18, 19, 20, 21, 22, 23, 25, 27, 30, 32, 36, 37, 38, 39, 40
2	MAPK10	Mitogen-activated protein kinase 10	2, 4, 15, 17, 18, 19, 20, 21, 22, 23, 24, 26, 27, 28, 32, 33, 37, 38, 40
3	PNP	Purine nucleoside phosphorylase	6, 7, 8, 9, 10, 12, 13, 16, 17, 19, 21, 22, 23, 24, 26, 27, 28, 29, 30
4	BMP2	Bone morphogenetic protein 2	28, 29, 30, 31, 32, 33, 34, 35, 36, 37, 38, 39, 40
5	GSTP1	Glutathione S-transferase P	3, 7, 8, 9, 10, 11, 12, 21, 23, 26, 28, 29, 30, 35
6	ITGAL	Integrin alpha-L	29, 30, 32, 33, 34, 35, 36, 37, 38, 39
7	AKR1C2	Aldo-keto reductase family 1 member C2	31, 32, 33, 34, 35, 36, 37, 38, 39, 40
8	MAPK8	Mitogen-activated protein kinase 8	2, 15, 17, 18, 19, 20, 21, 22, 23
9	CASP3	Caspase-3	1, 3, 9, 11, 12, 36, 37, 38
10	KDR	Vascular endothelial growth factor receptor 2	2, 4, 18, 33, 35, 36, 37, 40
11	BACE1	Beta-secretase 1	2, 4, 5, 15, 18, 38, 39, 40
12	MTAP	S-methyl-5'-thioadenosine phosphorylase	7, 9, 11, 13, 14, 16
13	CFB	Complement factor B	15,17, 20, 22, 24, 27
14	SELP	P-selectin	28, 29, 30, 31, 32, 33
15	PIM1	Serine/threonine-protein kinase pim-1	5, 23, 38, 40
16	MAPK1	Mitogen-activated protein kinase 1	1, 3, 9, 12, 20
17	CA1	Carbonic anhydrase 1	12, 13, 18, 31
18	EGFR	Epidermal growth factor receptor	1, 5, 6, 14
19	AMY1A	Alpha-amylase 1	2, 7, 16, 18
20	PDE4B	cAMP-specific 3',5'-cyclic phosphordiesterase 4B	10, 11, 14
21	NUDT9	ADP-ribose pyrophosphatase, mitochondrial	7, 32
22	CHEK1	Serine/threonine-protein kinase Chk1	13,14
23	MAPK14	Mitogen-activated protein kinase 14	4, 22
24	TGFBR2	TGF-beta receptor type-2	4, 34
25	AR	Androgen receptor	15,39
26	MAPKAPK2	MAP kinase-activated protein kinase 2	19, 20
27	CDK2	Cyclin-dependent kinase 2	5, 12
28	CSNK2A1	Casein kinase II subunit alpha	3, 8
29	F2	Prothrombin	2, 32
30	CDK5R1	Cyclin-dependent kinase 5 activator 1	6, 16
31	PDE5A	cGMP-specific 3',5'-cyclic phosphodiesterase	4
32	ICAM2	Intercellular adhesion molecule 2	7
33	TGFBR1	TGF-beta receptor type-1	10
34	CFD	Complement factor D	10
35	CA12	Carbonic anhydrase 12	11
36	PPARG	Peroxisome proliferator-activated receptor gamma	24
37	CASP7	Caspase-7	39
38	SRC	Proto-oncogene tyrosine-protein kinase Src	1

and pathways (Figure 6). Though the network diagram, a preliminary mechanism of the anti-RA of *P. hookeri* was obtained.

Table 3 show that the MAPK signaling pathway was involved in the largest number of targets. This pathway affects the release of inflammatory cytokines, and inhibits abnormal synaptic proliferation, thereby inhibition of RA bone erosion [25]. In addition, some cancer-related pathways were found, including those related to colorectal, prostate, and pancreatic cancers. This is consistent with a previous report [24].

DISCUSSION

The technique of UPLC-Q-TOF/MS has the pre-ponderances of fast analysis, low detection limit and strong qualitative ability. It has been widely used in the analysis of the chemical composition of medicinal plants, and has become an important means of identifying various compounds. In the MS data analysis process, it is extremely important to identify the correct quasi-molecular ion. This is related to the accuracy of the results. In the ESI+ mode, the quasi-molecular ion $[M+Na]^+$is easily formed, while the ESI- mode mainly forms the $[M-H]^-$ quasi-molecular ion, and the difference between

Table 3: The 44 biocarta pathways regulated by *P. hookeri* ($p < 0.01$)

No.	Pathway	Count	*P*-value	q-value	Gene
1	MAPK signaling pathway	10	2.42E-10	2.15E-09	MAPK1;CASP3;EGFR;TGFBR1;MAPK10;MAPK8; MAPK14;TGFBR2;MAPKAPK2
2	Adherens junction	7	2.69E-10	2.15E-09	MAPK1;SRC;EGFR;TGFBR1;CSNK2A1;TGFBR2
3	Colorectal cancer	7	4.17E-10	2.73E-09	MAPK1;CASP3;EGFR;TGFBR1;MAPK10;MAPK8; TGFBR2
4	Prostate cancer	7	5.81E-10	3.49E-09	MAPK1;EGFR;GSTP1;AR;CDK2
5	Epithelial cell signaling in Helicobacter pylori infection	6	6.58E-09	2.96E-08	SRC;CASP3;EGFR;MAPK10;MAPK8;MAPK14
6	Pancreatic cancer	6	8.50E-09	3.60E-08	MAPK1;EGFR;TGFBR1;MAPK10;MAPK8;TGFBR2
7	GnRH signaling pathway	6	8.54E-08	2.56E-07	MAPK1;SRC;EGFR;MAPK10;MAPK8;MAPK14
8	Focal adhesion	7	2.06E-07	5.49E-07	MAPK1;SRC;EGFR;MAPK10;KDR;MAPK8
9	VEGF signaling pathway	5	4.83E-07	1.22E-06	MAPK1;SRC;KDR;MAPK14;MAPKAPK2
10	ErbB signaling pathway	5	9.50E-07	1.91E-06	MAPK1;SRC;EGFR;MAPK10;MAPK8
11	TGF-beta signaling pathway	5	9.50E-07	1.91E-06	MAPK1;BMP2;TGFBR1;TGFBR2
12	Insulin signaling pathway	5	9.19E-06	1.32E-05	MAPK1;MAPK10;MAPK8
13	Complement and coagulation cascades	4	1.19E-05	1.52E-05	CFD;CFB;F2
14	Purine metabolism	5	1.47E-05	1.79E-05	PDE4B;PDE5A;PNP;NUDT9
15	Nitrogen metabolism	3	1.54E-05	1.84E-05	CA2;CA1;CA12
16	Cytokine-cytokine receptor interaction	6	1.56E-05	1.84E-05	BMP2;EGFR;TGFBR1;KDR;TGFBR2
17	Fc epsilon RI signaling pathway	4	2.04E-05	2.29E-05	MAPK1;MAPK10;MAPK8;MAPK14
18	Alzheimer's disease	5	3.05E-05	3.24E-05	CASP7;MAPK1;CASP3;BACE1;CDK5R1
19	Toll-like receptor signaling pathway	4	5.57E-05	5.42E-05	MAPK1;MAPK10;MAPK8;MAPK14
20	Type II diabetes mellitus	3	1.05E-04	9.30E-05	MAPK1;MAPK10;MAPK8
21	Endometrial cancer	3	1.61E-04	1.29E-04	MAPK1;EGFR
22	Starch and sucrose metabolism	3	1.61E-04	1.29E-04	AMY1B;AMY1A;AMY1C
23	Natural killer cell mediated cytotoxicity	4	1.79E-04	1.38E-04	MAPK1;CASP3;ITGAL;ICAM2
24	Non-small cell lung cancer	3	1.81E-04	1.38E-04	MAPK1;EGFR
25	p53 signaling pathway	3	3.73E-04	2.36E-04	CASP3;CDK2;CHEK1
26	Chronic myeloid leukemia	3	4.77E-04	2.83E-04	MAPK1;TGFBR1;TGFBR2
27	Gap junction	3	8.93E-04	4.34E-04	MAPK1;SRC;EGFR
28	Regulation of actin cytoskeleton	4	0.001005	4.79E-04	MAPK1;EGFR;ITGAL;F2
29	Urea cycle and metabolism of amino groups	2	0.001458	6.32E-04	MTAP
30	Thyroid cancer	2	0.001564	6.66E-04	PPARG;MAPK1
31	Cell cycle	3	0.001814	7.42E-04	CDK2;CHEK1
32	Cell adhesion molecules (CAMs)	3	0.002542	0.001011	SELP;ITGAL;ICAM2
33	Bladder cancer	2	0.003261	0.001255	MAPK1;EGFR
34	Wnt signaling pathway	3	0.003625	0.001388	MAPK10;MAPK8;CSNK2A1
35	mTOR signaling pathway	2	0.004957	0.001844	MAPK1
36	Amyotrophic lateral sclerosis (ALS)	2	0.005727	0.002082	CASP3;MAPK14
37	Hedgehog signaling pathway	2	0.005927	0.002144	BMP2
38	Acute myeloid leukemia	2	0.006338	0.002259	MAPK1;PIM1
39	Glioma	2	0.007645	0.002711	MAPK1;EGFR
40	Adipocytokine signaling pathway	2	0.008105	0.002819	MAPK10;MAPK8
41	PPAR signaling pathway	2	0.008818	0.003045	PPARG
42	Metabolism of xenobiotics by cytochrome P450	2	0.008818	0.003045	GSTP1;AKR1C2
43	Melanoma	2	0.009062	0.003107	MAPK1;EGFR
44	Drug metabolism - cytochrome P450	2	0.009309	0.003169	GSTP1

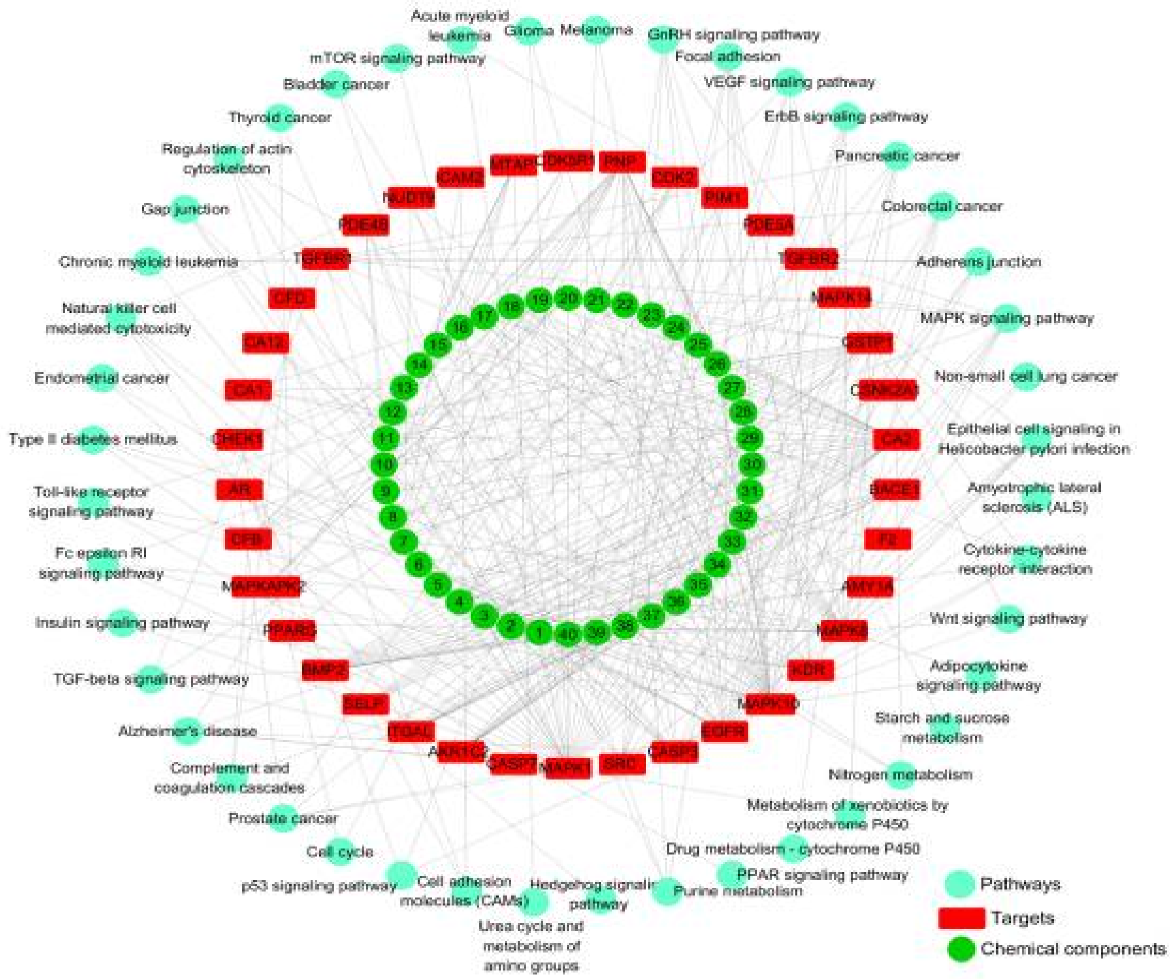

Figure 6: The “component-target-pathway” network of *P. hookeri*

[M+Na]$^+$ and [M-H]$^-$ is 24 Da. It can be judged that the ion is a quasi-molecular ion. In the present study, UPLC-Q-TOF/MS technique was used to analyze the chemical components of *P. hookeri*. The results of this study provide a basis for research on the pharmacodynamics and quality control of *P. hookeri*.

It is evident from the results obtained in this study that CA2, MAPK10 and PNP were associated with most of the compounds. Therefore, these factors can be considered to be the main targets. The CA2 gene encodes carbonic anhydrase 2, which is crucial for bone resorption and osteoclast differentiation, and the pathway involved is nitrogen metabolism. There is an imbalance in nitrogen metabolism in patients with RA. However, most patients with RA are in positive nitrogen balance when nitrogen intake is adequate [26]. Purine nucleoside phosphorylase is encoded by PNP gene, and it catalyzes the phosphorolytic cleavage of the N-glycosidic linkage in purine (deoxy) ribonucleosides, with the liberation of free purine base and pentose-1-phosphate. The pathway involved is purine metabolism. Purine metabolism has a highly synergistic effect on immune cell function in RA [27]. The MAPK10 gene encodes mitogen-activated protein kinase 10, which is associated with inflammation and immune function [28]. The pathways related to RA include MAPK, VEGF, TGF-beta signaling pathway, and focal adhesion. Results from network pharmacological prediction showed that one compound can act on one or more different targets, and one target can also act on different pathways, suggesting that anti-RA property of *P. hookeri* involves multiple components, multiple targets, and multiple pathways.

The network pharmacology method used in this study is an innovative methodology due to the establishment of multilayer networks of disease - target-drug for forecasting drug targets in an integral manner, and for boosting efficient drug discovery [29]. This method represents a breakthrough, when compared with the traditional herbal medicine research methodology of gene-target-disease, and initiates a new system of multiple genes-multiple targets-complex diseases.

This is the first study on the mechanism involved in the anti-RA effect of *P. hookeri*, and the first to use the novel technique of network pharmacology. Using this method, the main targets and pathways were successfully predicted, thereby providing a foundation for further research. This method is important for the study of complex drugs and should be applied in future studies.

CONCLUSION

A UPLC-Q-TOF/MS method has been successfully developed for the rapid analysis of chemical components of *P. hookeri*. A total of 40 compounds have been identified. Network pharmacology method enables the prediction of the therapeutic effect of *P. hookeri* on RA via a mechanism involving multiple components, multiple targets and multiple pathways.

DECLARATIONS

Acknowledgement

The authors gratefully acknowledge the financial support from National Natural Science Foundation of China (no. 81274193), and Construction Plan of Scientific Research Innovation Team in Sichuan Province (no. 11TD004).

Conflict of interest

The authors declare that no conflict of interest is associated with this work.

Contribution of authors

The authors declare that this work was done by the authors named in this article and all liabilities pertaining to claims relating to the content of this article will be borne by them. Ce Tang and Yi Zhang conceived and designed the experiments; Ce Tang, Hai-Jiao Li, Gang Fan, and Ting-Ting Kuang performed the experiments; Ce Tang and Yi Zhang wrote the paper; Ce Tang, Ting-Ting Kuang, Xian-Li Meng, and Zhong-Mei Zou analyzed the data. All authors reviewed the manuscript.

REFERENCES

1. *Maijer KI, Gudmann NS, Karsdal MA, Gerlag DM, Tak PP, Bay-Jensen AC. Neo-Epitopes—Fragments of Cartilage and Connective Tissue Degradation in Early Rheumatoid Arthritis and Unclassified Arthritis. Plos One 2016; 11(3): e0149329.*
2. *Yang J, Zuo F, Wei ZC, Zeng Y, Meng XL, Zhang Y. Therapeutic Effects and Mechanisms of Total Glucosides of Herba Pterocephali on Adjuvant Arthritis Rats. Tradit Chin Drug Res Pharmaco 2016; 27(6): 788-794.*
3. *Yangben ZX, Pengmao DZ, Xin CJ, Zhuoma CD, Gong B. Clinical Evaluation of Tibetan Medicine in Treating Rheumatoid Arthritis. J Med Pharm Chin Minorities 2013; 5: 18-19.*
4. *Ri S, Zhou XB. Clinical observation of 101 cases of rheumatoid arthritis treated by Tibetan medicine. J Med Pharm Chin Minorities 2017; 12: 36-37.*
5. *Tang C, Fan G, Li Q, Su JS, Meng XL, Zhang Y. Simultaneous determination of ten compounds in two main medicinal plant parts of Tibetan herb, Pterocephalus hookeri (CB Clarke) Höeck, by ultra-high performance liquid chromatography-photodiode array. Trop J Pharm Res 2017; 16 (6): 1407-1416.*
6. *Tian J, Wu FE, Qiu MH, Nie RL. Triterpenoid saponins from Pterocephalus hookeri. Phytochem 1993; 32 (6): 1535-1538.*
7. *Wang J, Zhao KH, Geng ZJ, Lai XR, Yang WJ, Hu XX, Zhang Y, Jiangrong SL. Comparison Study on Zhenbu Disease of Tibetan Medicine and Bi Syndrome in Traditional Chinese Medicine. Modern Tradit Chin Med Mater Med-World Sci Technol 2015; 17(10): 2167-2171.*
8. *Zhang L, Hu JJ, Lin JW, Fang WS, Du GH. Anti-inflammatory and analgesic effects of ethanol and aqueous extracts of Pterocephalus hookeri (C.B. Clarke) Höeck. J Ethnopharmacol 2009; 123 (3): 510-514.*
9. *Shen XF, Zeng Y, Li JC, Tang C, Zhang Y, Meng XL. The anti-arthritic activity of total glycosides from Pterocephalus hookeri, a traditional Tibetan herbal medicine. Pharm Biol 2017; 55(1): 560-570.*
10. *Wu L, Wang Y, Nie J, Fan X, Cheng Y. A network pharmacology approach to evaluating the efficacy of Chinese medicine using genome-wide transcriptional expression data. Evid Based Complement Alternat Med 2013; 2013: 915343.*
11. *Zhang JF, Huang S, Shan LH, Chen L, Zhang Y, Zhou XL. New Iridoid Glucoside from Pterocephalus hookeri. J Ogr Chem. 2015; 35: 2441-2444.*
12. *Huang S, Zhang JF, Shan LH, Zhang Y, Zhou XL. A novel tetrairidoid glucoside from Pterocephalus hookeri. Heterocycles 2017; 94(3): 485.*
13. *Qi LW, Chen CY, Li P. Structural characterization and identification of iridoid glycosides, saponins, phenolic acids and flavonoids in Flos Lonicerae Japonicae by a fast liquid chromatography method with diode-array detection and time-of-flight mass spectrometry. Rapid Commun Mass Spectrom 2009; 23(19): 3227-3242.*
14. *Sun HY, Liu MX, Lin ZT, Jiang HX, Niu YY, Wang H, Chen SZ. Comprehensive identification of 125 multifarious constituents in Shuang-huang-lian powder*

injection by HPLC-DAD-ESI-IT-TOF-MS. J Pharm Biomed Anal 2015; 115: 86-106.

15. *Ling Y, Liu KY, Zhang Q, Liao L, Lu YH. High performance liquid chromatography coupled to electrospray ionization and quadrupole time-of-flight–mass spectrometry as a powerful analytical strategy for systematic analysis and improved characterization of the major bioactive constituents from Radix Dipsaci. J Pharm Biomed Anal 2014; 98: 120-129.*
16. *Tian XY, Wang YH, Liu HY, Yu SS, Fang WS. On the Chemical Constituents of Dipsacus asper. Chem Pharm Bull 2007; 55(12): 1677-1681.*
17. *Prasad D, Juyal V, Singh R, Singh V, Pant G, Rawat MS. A new secoiridoid glycoside from Lonicera angustifolia. Fitoterapia 2000; 71(4): 420-424.*
18. *Wu YC, Yin YJ, Li YM, Guo FJ, Zhu GF. Secoiridoid/iridoid subtype bis-iridoids from Pterocephalus hookeri. Maqn Reson Chem 2014; 52(11): 734-738.*
19. *Gülcemal D, Masullo M, Alankuş-Calişkan O, Karayildirim T, Senol SG, Piacente S, Bedir E. Monoterpenoid glucoindole alkaloids and iridoids from Pterocephalus pinardii. Maqn Reson Chem 2010; 48(3): 239-243.*
20. *Tian J, Wu FE, Qiu MH, Nie RL. Triterpenoid saponins from Pterocephalus hookeri. Phytochem 1993; 32 (6): 1535-1538.*
21. *Zhang Y, Li WJ, Meng XL, Shen P, Jia MR. Chemical Constituents of Tibet Drug Pterocephalus hookeri (C. B. Clarke) Hoeck. J Chengdu Univ Tradit Chin Med 2002; 25(3): 41-42.*
22. *Tian J, Wu FE, Qiu MH, Nie RL. Two triterpenoid saponins from Pterocephalus bretschneidri. Phytochem 1993; 32(6): 1539-1542.*
23. *Tang C, Su JS, Yang J, Zuo F, Meng XL, Zou ZM, Zhang Y. Content Determination of Oleanolic Acid and Ursolic Acid from Different Medicinal Parts in Tibetan Medicine Pterocephalus hookeri by UPLC-PDA. J China Pharm 2017; 28(7): 929-932.*
24. *Guo CX, Wu YC, Zhu YZ, Wang YC, Tian LL, Lu Y, Han C, Zhu GF. In Vitro and In Vivo Antitumor Effects of n-Butanol Extracts of Pterocephalus hookeri on Hep3B Cancer Cell. Evid Based Complement Alternat Med 2015; 2015: 159132.*
25. *Zuo F, Wei T, Tong D, Zhang Y, Chen XR, Zeng Y. Pharmacodynamic mechanism of modified Ganlu Yaoyu San in treatment of rheumatoid arthritis based on MAPK signaling pathway. Chin J Chin Mater Med 2017; 42(7): 1245-1250.*
26. *Clark WS, Bauer W, Appleton J, Manning E. The Relationship of Alterations in Mineral and Nitrogen Metabolism to Disease Activity in a Patient. Acta Rheumatol Scand 1956; 2(4): 193-212.*
27. *Morgan SL, Oster RA, Lee JY, Alarcón GS, Baggott JE. The effect of folic acid and folinic acid supplements on purine metabolism in methotrexate-treated rheumatoid arthritis. Arthritis Rheum 2004; 50(10): 3104-3111.*
28. *Vargas-Alarcón G, Posadas-Romero C, Villarreal-Molina T, Alvarez-León E, Angeles-Martinez J, Posadas-Sanchez R, Monroy-Muñoz I, Luna-Fuentes S, González-Salazar C, Ramirez-Bello J, et al. IL-24 gene polymorphisms are associated with cardiometabolic parameters and cardiovascular risk factors but not with premature coronary artery disease: the genetics of atherosclerotic disease Mexican study. J Interferon Cytokine Res 2014; 34(9): 659-666.*
29. *Ma XH, Lv B, Li P, Jiang XQ, Zhou Q, Wang XY, Gao XM. Identification of "Multiple Components-Multiple Targets-Multiple Pathways" Associated with Naoxintong Capsule in the Treatment of Heart Diseases Using UPLC/Q-TOF-MS and Network Pharmacology. Evid Based Complement Alternat Med 2016; 2016: 9468087.*